NASA Contractor Report 177990

NASA-CR-177990
19860001831

INTERACTION OF MIXED MODE LOADING
ON CYCLIC DEBONDING IN ADHESIVELY
BONDED COMPOSITE JOINTS

S. Mall, M. A. Rezaizadeh,
and G. Ramamurthy

UNIVERSITY OF MISSOURI
Rolla, Missouri

NASA

National Aeronautics and
Space Administration

Langley Research Center
Hampton, Virginia 23665

NF01016

INTERACTION OF MIXED MODE LOADING ON CYCLIC DEBONDING IN ADHESIVELY BONDED COMPOSITE JOINTS

S. Mall
M. A. Rezaizadeh
G. Ramamurthy
Department of Engineering Mechanics
University of Missouri
Rolla, Missouri

ABSTRACT

A combined experimental and analytical investigation of an adhesively bonded composite joint was conducted to characterize the fracture mode dependence of cyclic debonding. The system studied consisted of graphite/epoxy adherends bonded with EC 3445 adhesive. Several types of specimens were tested which provided the cyclic debond growth rate measurements under various load conditions: mode I, mixed mode I-II, and almost mode II. This study showed that the total strain-energy-release rate was the governing factor for cyclic debonding.

NOMENCLATURE

a	length of debond
$\dfrac{da}{dN}$	debond growth rate
c, n	curve-fit parameters
E	Young's modulus of adhesive
E_1, E_2	Young's moduli of composite
G	shear modulus of adhesive
G_{12}	shear modulus of composite
G_I	mode I strain-energy-release rate
G_{II}	mode II strain-energy-release rate
G_T	total strain-energy-release rate $(= G_I + G_{II})$
N	number of cycles
ν	Poisson's ratio of adhesive
ν_{12}, ν_{23}	Poisson's ratio of composite

INTRODUCTION

Adhesive bonding is a very desirable method for joining composite components to achieve the maximum weight advantage without any strength degradation of basic laminate due to fasteners holes. If the advantages of adhesively bonded composite joints are to be fully exploited, a better understanding of their fatigue failure mechanism is needed. When an adhesively bonded joint is subjected to fatigue load, one of the several possible damage modes that can occur is the progressive separation of bond between adherends. This is commonly referred to as cyclic debonding. Basic concepts from fracture mechanics have proven successful in modeling cyclic debonding ([1-4]). In a previous study ([5]) by Mall et al., cyclic debonding of adhesively bonded composite joints was investigated with the cracked-lap-shear (CLS) specimen. Two different geometries provided the different G_I to G_{II} ratios where G_I is the strain-energy-release rate for opening mode I and G_{II} for sliding mode II. Data from these two specimens were used to determine the fracture mode dependence of cyclic debonding. The cyclic debond growth rate correlated better with the total strain-energy-release rate G_T than it did with either G_I or G_{II} independently ([5]).

The previous study ([5]) was, later on, extended to investigate cyclic debonding under opening mode I load with double-cantilever-beam (DCB) specimen ([6]). The relations G_T versus da/dN from the DCB specimens and G_T versus da/dN from the CLS specimens agreed with each other, where G_T is total (and also opening mode I) strain-energy-release rate for DCB specimens, and G_T is total strain-energy-release rate for CLS specimens. The relation G_T versus da/dN from the CLS specimen under mixed mode loading did not, however, agree with the relation G_T versus da/dN from the DCB specimen under the opening mode I loading. The results of this study ([6]), thus, suggested that the cyclic debond failure in the adhesively bonded composite joints is governed by total strain-energy-release rate.

Since the previous study ([5]) used two geometries of CLS specimen which provided a rather narrow range of mixed mode loading (i.e. G_I/G_{II} ranged from 0.25 to 0.31), further study was considered appropriate to investigate the interaction of mixed mode loading on cyclic debonding. For this purpose, three new geometries of cracked-lap-shear specimen were tested, which provided G_I/G_{II} ranging from 0 to 0.38. The present paper provides the details and results of this study. Further, the data obtained from the present study as well

as from previous studies (5,6) gave a wide range of mixed mode loading conditions for evaluation of the mechanics of cyclic debonding in adhesively bonded composite joints.

SPECIMEN PREPARATION AND CONFIGURATION

The cracked-lap-shear specimen, shown in Fig. 1, was employed, because it represents a simple structural joint subjected to in-plane loading. Both shear and peel stresses are present in the bond line of this joint. The magnitude of each component of this mixed mode loading can be modified by changing the relative thicknesses of strap and lap adherends (7). In the previous study (5), two geometries of CLS specimens (i.e. lap of 8 plies bonded to strap of 16 plies[1] and lap of 16 plies bonded to strap of 8 plies[2]) were tested. These two geometries provided the uniform G_I to G_{II} ratios of 0.25 and 0.31 over the region of debond length measurement from 0 to 115 mm.
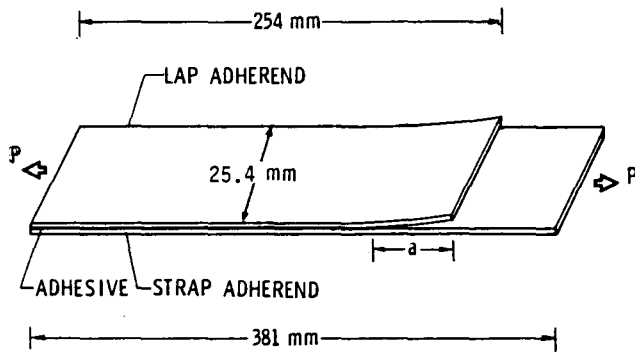

Figure 1. Cracked-Lap-Shear Specimen

The present study employed the same cracked-lap-shear specimen design described above, except that strap and lap adherends had 16 or 32 plies. This arrangement provided two types of specimen: (1) lap adherend of 16 plies bonded to strap adherend of 32 plies[3], and (2) lap adherend of 32 plies bonded to strap adherend of 16 plies[4]. These geometries provided the variation of G_I to G_{II} ratio ranging from 0.03 to 0.38, as discussed in a later section. The lengths of strap and lap adherends were 381 and 254 mm, respectively (a total of 127 mm was for grip support on both ends).

The tapered-cracked-lap-shear specimen shown in Fig. 2 was also used in the present study. This specimen had lap of 16 plies bonded to the strap of 8 plies. The lap adherend was machined to obtain a taper angle of 5° as shown in Fig. 2. The lengths of strap and lap adherends were 381 and 241 mm, respectively (a total of 127 mm was for grip support on both ends). The width of tapered-cracked-lap shear specimen was 25 mm. The G_I/G_{II} varied from 0.0 to 0.07 in this specimen, as discussed in a later section.

The bonded system consisted of graphite/epoxy (T300/5208) adherends bonded with EC-3445 adhesive. The EC-3445 adhesive is a thermosetting paste with a cure temperature of 121°C. Specimens were fabricated

---

[1] Will be referred to as 16/8 in the figures.

[2] Will be referred to as 8/16 in the figures.

[3] Will be referred to as 32/16 in the figures.

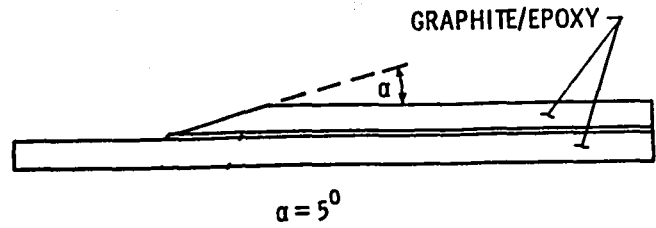[4] Will be referred to as 16/32 in the figures.

$$a = 5^0$$

Figure 2. Tapered-Cracked-Lap-Shear Specimen

by conventional secondary bonding procedure. The bonding process followed the manufacturer's recommended procedure. The nominal adhesive thickness was 0.10 mm. The composite adherends consisted of quasi-isotropic layups of $[0/45/-45/90]_S$, $[0/45/-45/90]_{2S}$ and $[0/45/-45/90]_{4S}$ with 0° ply at the adherend-adhesive interface.

TESTING PROCEDURE

The objective of the test program was to measure the debond growth rate under the fatigue loading. The fatigue test of all specimens were conducted in a servo-hydraulic test machine at a cyclic frequency of 10 Hz. In all tests, constant amplitude cyclic loads were applied at a stress ratio of 0.1. Debond lengths and fatigue cycles were monitored continuously throughout the test. The measured relation between the debond length and fatigue cycle provided the debond growth rate, da/dN. Tests were conducted at two or more constant amplitude stress levels to get several values of debond growth rates from each specimen. As it will be explained in the section entitled "FINITE ELEMENT ANALYSIS", the strain-energy-release rates, G_T, G_I and G_{II} were not uniform over the region of debond length measurement. Therefore, for each applied stress level, the measured debond data were fitted with a polynomial curve using regression analysis which, then provided the debond growth rates. Figure 3 shows a typical relation between the measured debond length and fatigue
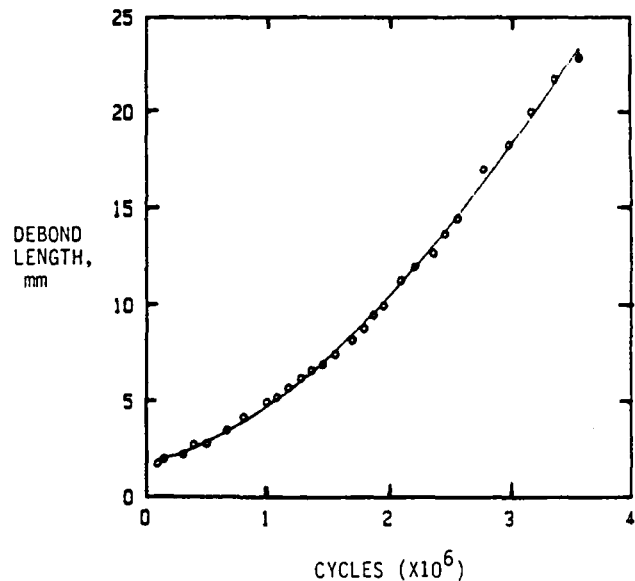

CYCLES (X10^6)

Figure 3. Relation Between Measured Debond Length and Fatigue Cycles in Tapered-Cracked-Lap-Shear Specimen
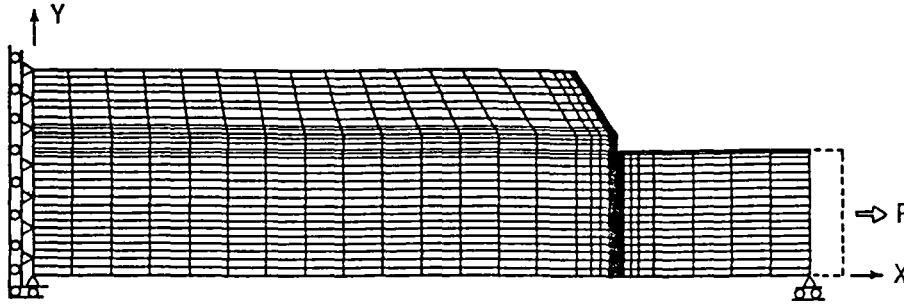
2

Figure 4. Finite Element Model (Scale: Y = 10X)

cycles in the tapered region of a tapered-cracked-lap-shear specimen where G_I/G_{II} varied from 0 to 0.07.

DEBOND SURFACES

The possible failure modes in a composite bonded joint are cyclic debonding, delamination, adherend fatigue, or a combination of these. All specimens in the present study failed by cyclic debonding of the adhesive. Although some adhesive remained on both the strap and lap adherends, significantly more adhesive remained on the lap adherend. On close examination of the debond surfaces, it was found that the debond was always closer to the strap than to the lap adherend. This debond behavior was similar to as observed in the previous study (5). A possible explanation for this debond characteristic was investigated with the finite element analysis (5). In this analysis, the strain-energy-release rates, G_T, G_I and G_{II} were calculated at the various debond locations within the thickness of adhesive. This analysis showed that G_T was constant for all locations of the debond, while G_I had its maximum value near the adhesive-strap interface and G_{II} had its maximum value near the adhesive-lap interface. The debond always initiated and grew in the region of highest G_I (near the adhesive-strap interface). This indicates that G_I has the greater influence on the de-

bond location in adhesive joint. This is consistent with the observations that adhesives are inherently weaker under peel loading than under shear loading.

FINITE ELEMENT ANALYSIS

The tested cracked-lap-shear specimens were analyzed with the finite element program GAMNAS (7) to determine the strain-energy-release rate for given geometry, debond length, and applied load. This two-dimensional analysis accounts for the geometric non-linearity associated with the large rotations in the unsymmetric cracked-lap-shear specimen.

A typical finite-element model of a tapered cracked-lap-shear specimen is shown in Fig. 4. This FEM mesh consisted of about 1600 isoparametric 4-node elements and had about 3000 degrees of freedom. Each ply of composite was modeled as a separate layer in the finite element model. A multipoint constraint was applied to the loaded end of the model to prevent rotation (i.e., all of the axial displacements along the ends are equal to simulate actual grip loading of the specimen). Plane-strain condition was assumed in the analysis. The material properties of composite adherends and adhesives are listed in Tables 1 and 2. The strain-energy-release rate was computed using a virtual crack-closure technique (8).
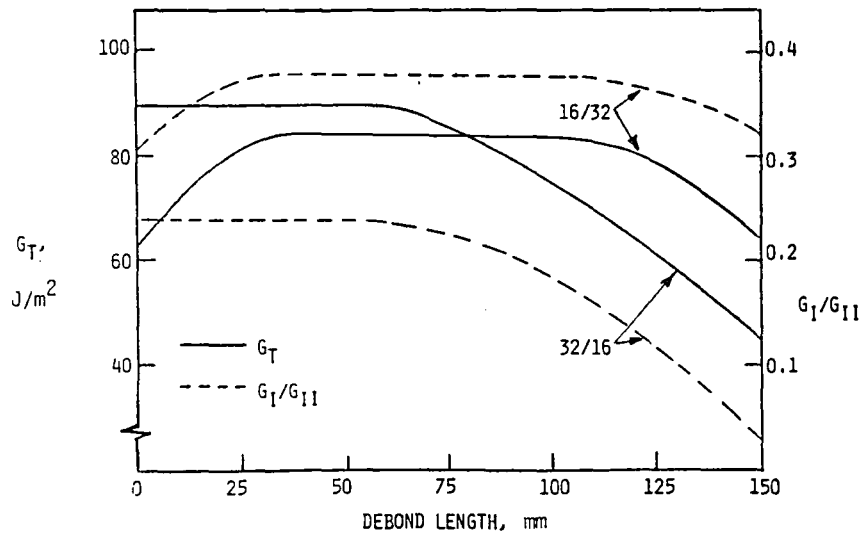

Figure 5. Variation of Strain-Energy-Release Rates with Debond Length for Applied Stress of 82 MPa

3

The previous study (5) indicated that at least 12 elements were required through the adhesive thickness to reach convergence on G_I and G_{II} calculations. However, the calculation of G_T was not affected by the number of elements through the adhesive thickness. Therefore, the adhesive was modeled with twelve layers of elements in the present study.

As mentioned previously, the debond grew near the interface of the adhesive and strap adherend in all tests. It was very difficult to measure the exact location of the debond, but in general the debond grew within one-fourth of the thickness of adhesive closest to interface. To analyze the experimental debond growth rates, the debond location for all calculations was selected by engineering judgement to be at one-sixth of the adhesive thickness away from the adhesive-strap interface.

Figure 5 shows the variation of strain-energy-release rates (G_T and G_I/G_{II}) with the debond length for the two geometries of CLS specimens without taper (i.e. lap of 16 plies bonded to strap of 32 plies and lap of 32 plies bonded to strap of 16 plies). Figure 6 shows the variation of strain-energy-release rates (G_T and G_I/G_{II}) with the debond length for the tapered-cracked-lap specimen having 5° taper angle.

RESULTS AND DISCUSSIONS

As previously mentioned, the objective of the present study was to determine the influence of components of strain-energy-release rate (G_T, G_I or G_{II}) on cyclic debonding under in-plane mixed-mode loading condition. The measured debond growth rates were, therefore, correlated with each of the calculated strain-energy-release rates G_I, G_{II}, and G_T. If one component of strain-energy-release rate had a dominant influence, it would correlate significantly better than the others when comparing the debond data from specimens with different G_I to G_{II} ratios.

In the previous study (5), two geometries of CLS specimens, consisting of lap of 8 plies bonded to strap of 16 plies and lap of 16 plies bonded to strap of 8 plies, were tested. These geometries provided the uniform G_I to G_{II} ratio of 0.31 and 0.25, respectively. The measured debond growth rates, da/dN, were correlated with G_T, G_I, and G_{II}. This correlation is shown in Fig.7 where an equation of the form
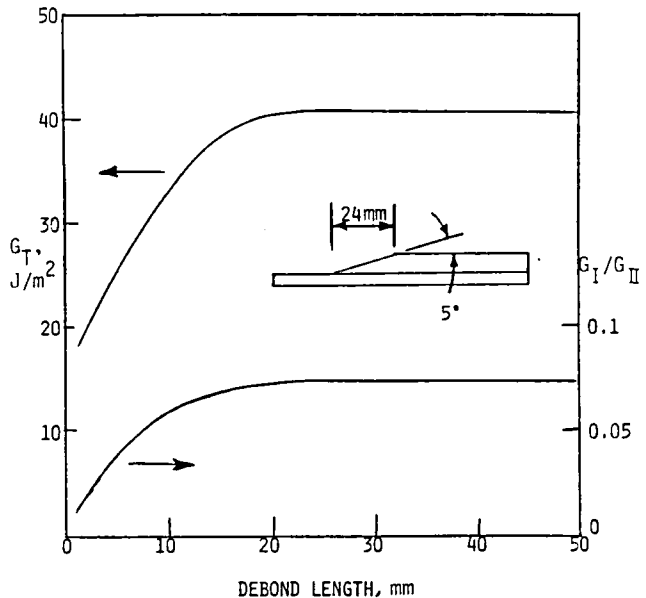

Figure 6. Variation of Strain-Energy-Release Rates with Debond Length for Applied Stress of 82 MPa
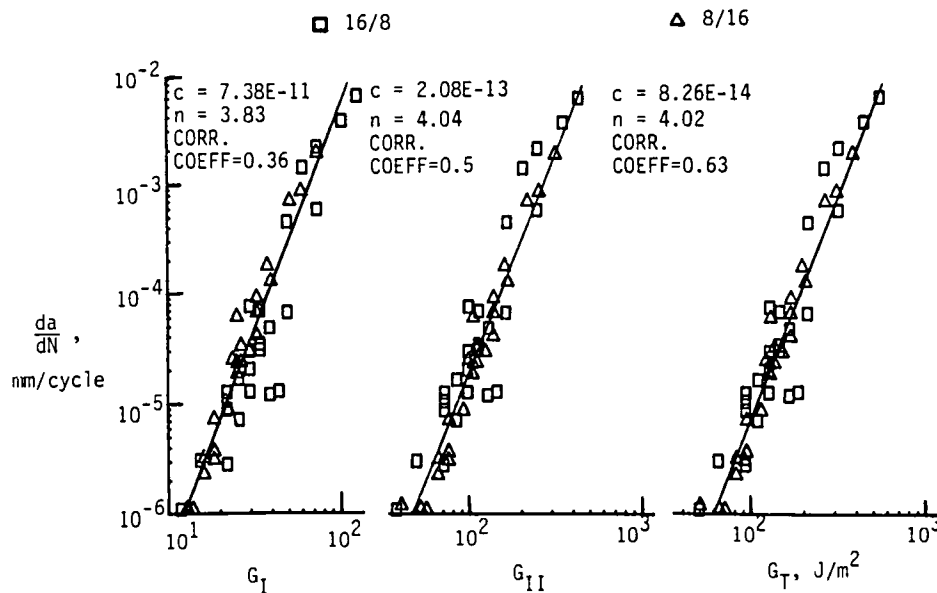

Figure 7.   Relation Between Strain-Energy-Release Rates and Debond Growth Rate from CLS Specimens

4

$$da/dN = c(G)^n \qquad\qquad (1)$$

was fitted to the data from both specimens. The solid line shows this power-law relationship in Fig. 7. Also, the values of c and n, as well as the correlation coefficient are shown in Fig. 7. Since the correlation coefficient closer to one is the indication of better correlation, the G_T correlated the debond growth rate better than either G_I or G_{II}. These results, therefore, suggested that the cyclic debond growth was a function of total strain-energy-release rate. However, this observation was based on a rather narrow range of G_I to G_{II} ratio, i.e. from 0.25 to 0.31.

The measured debond growth rate obtained from three geometries of CLS specimen, tested in the present study, were correlated with strain-energy-release rates G_T, G_I and G_{II} as shown in Figs. 8 and 9. These figures also show the relation between strain-energy-release rates and debond growth rate from two geometries of CLS specimen tested in the previous study (5). These relations are shown in Figs. 8 and 9 as
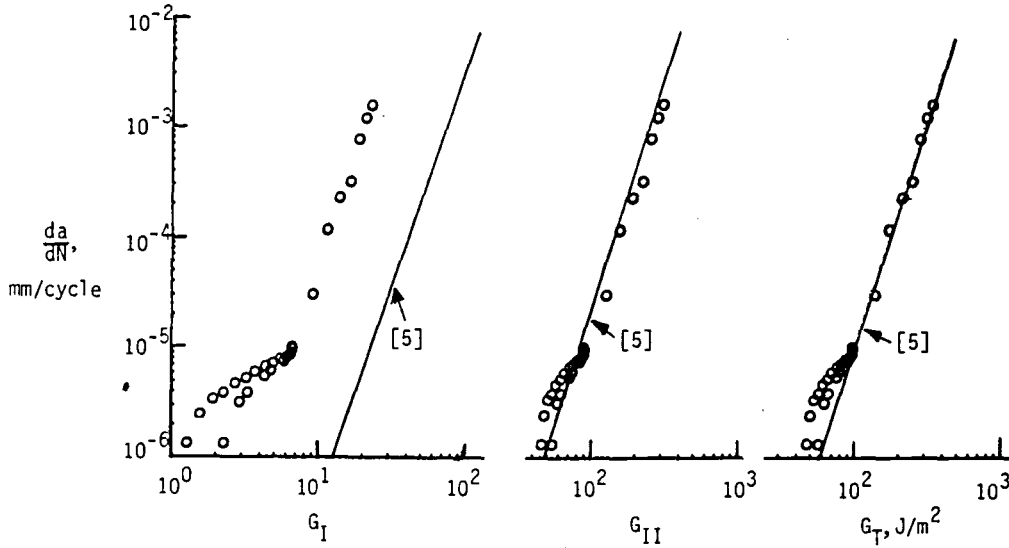

Figure 8. Relation Between Strain-Energy-Release Rates
and Debond Growth Rate from Tapered-Cracked-Lap-Shear Specimen
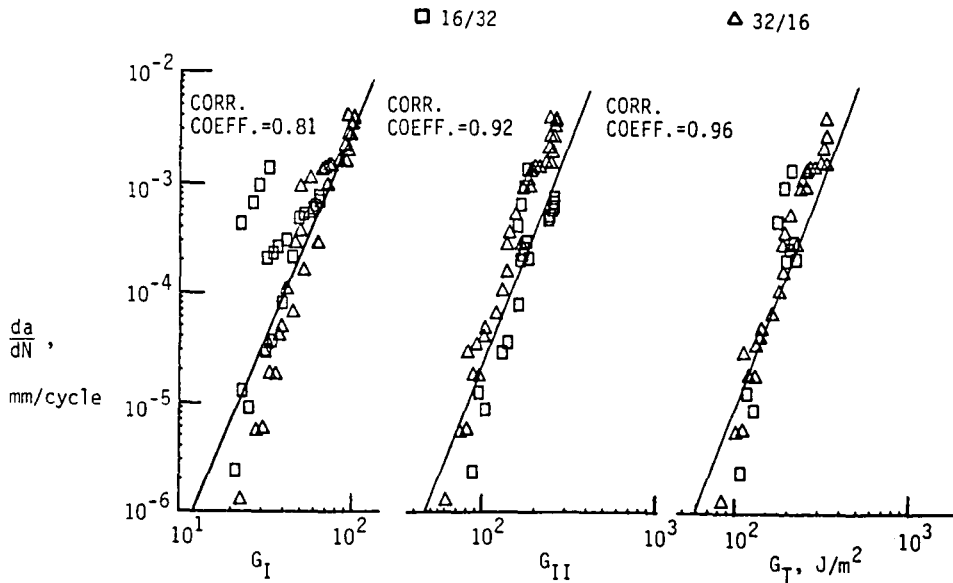

Figure 9. Relation Between Strain-Energy-Release Rates
and Debond Growth Rate from CLS Specimens

solid line instead of data points for the sake of clarity. In the present study, the debond growth rates were measured over the range of G_I/G_{II} varying from 0 to 0.38.

The measured debond growth rates from tapered-cracked-lap-shear specimens were correlated with strain-energy-release rates G_T, G_I and G_{II} as shown in Fig. 8. The corresponding relations obtained from the previous study (5) are also shown in Fig. 8 as solid line. The G_T versus da/dN from the tapered-cracked-lap shear specimen are in good agreement with G_T versus da/dN relationship from the CLS specimen (5), and also G_{II} versus da/dN relations from both specimens are in agreement with each other. On the other hand, the G_I versus da/dN relations from both specimens did not agree, as shown in Fig. 8. In case of tapered-cracked-lap shear specimen, the G_I to G_{II} ratios varied from 0 to 0.07, i.e. debond grew predominantly under sliding mode II condition. The peel stress, and hence G_I, is zero for all practical purposes in the tapered-cracked-lap shear specimen. Further, G_T is almost equal to G_{II} in the tapered-cracked-lap shear specimen. Figure 8, thus, clearly indicates that the cyclic debond growth is a function of total strain-energy-release rate.

Figure 9 shows the relations between strain-energy-release rates and debond growth rate obtained from two geometries of cracked-lap-shear specimen without taper in the present study. These two geometries, as described previously, consisted of lap of 16 plies bonded to strap of 32 plies and lap of 32 plies bonded to strap of 16 plies which provided G_I/G_{II} ranging from 0.03 to 0.38 as shown in Fig. 5. These two geometries of CLS specimen provided the debond growth rate measurements in the mixed mode loading condition which is a typical loading condition for the real life structural joints. The strain-energy-release rates (G_T, G_I and G_{II}) versus da/dN data from the CLS specimen of the present study are in good agreement with their counterparts obtained in the previous study (5) shown as solid lines in Fig. 9. Further, debond growth rate data from these two specimens in the present study correlated better with G_T than with either G_I or G_{II} as shown by the correlation coefficients in Fig. 9. This is similar to that found in the previous study (5). Therefore, this confirms that debond growth rate is a function of the combined effects of G_I and G_{II}. Furthermore, Figs. 7, 8 and 9 show that data from different specimen geometries are within an acceptable scatter band (similar to that observed in fatigue crack propagation in metals). This indiates that specimen geometry did not influence the relationship between the debond growth rate and total strain-energy-release rate, G_T.

In a previous study (6), the cyclic debonding was investigated under opening mode I load with double-cantilever-beam specimen. The measured debond growth rates from DCB specimens were correlated with the corresponding strain-energy-release rate, G_I as shown in Fig. 10. Figure 10 also shows G_T versus da/dN and G_I versus da/dN relations from the CLS specimens under mixed mode loading (5). The CLS data points are not shown herein for the sake of clarity. The G_I versus da/dN data from the DCB specimen are in good agreement with the G_T versus da/dN relationship from the CLS specimen, represented by the solid line. On the other hand, the G_I versus da/dN relationship from the CLS specimen represented by the dashed line, did not agree with the DCB specimen. This further shows that the cyclic debond growth is a function of total strain-energy-release rate. In a previous study (9), it has been also shown that total strain-energy-release rate

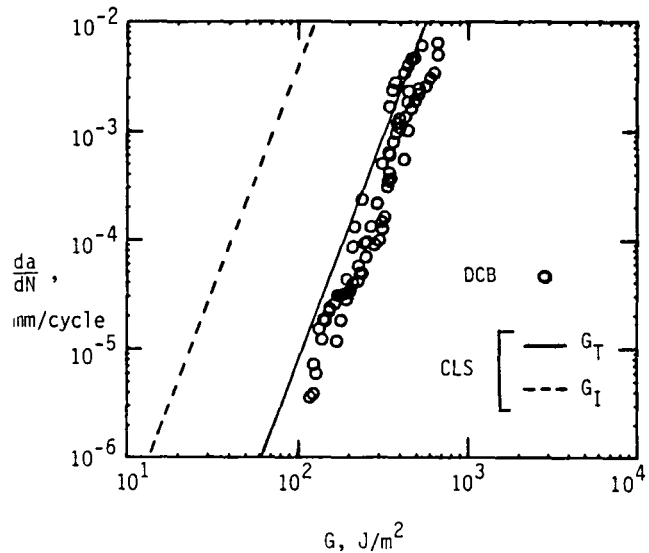was the parameter which governed the intiation of cyclic debonding.

Figure 10. Relation Between Strain-Energy-Release Rates and Debond Growth Rate from DCB and CLS Specimens

Table 1. Adhesive Material Properties

	Modulus, GPa		Poisson's Ratio
	E	G	ν
EC-3445 (3M Company)	1.81	0.65	0.4

Table 2. Graphite/Epoxy[a] Adherend Material Properties

Modulus,[b] GPa			Poisson's Ratio[b]	
E_1	E_2	G_{12}	ν_{12}	ν_{23}
131.0	13.0	6.4	0.34	0.35

[a]T300/5208 (NARMCO), fiber volume fraction is 0.63.

[b]The subscripts 1, 2 and 3 corresond to the longitudinal, transverse, and thickness directions, respectively, or a unidirectional ply.

CONCLUSION

A combined experimental and analytical investigation of composite-to-composite bonded joints was undertaken to characterize the influence of components of strain-energy-release rate (G_T, G_I or G_{II}) on cyclic debonding under mixed mode loading. The system studied consisted of graphite/epoxy adherends bonded with EC 3445 adhesive. Several types of specimens were tested which provided the debond growth rate measurements under various load conditions: mode I, mixed mode I-II, and almost mode II loadings. This study led to the following conclusion:

'The total strain-energy-release rate is the governing factor for cyclic debonding in adhesively bonded composite joints when subjected to in-plane mixed mode loading.'

This should be, however, verified further for several structural adhesives and various loading conditions.

ACKNOWLEDGEMENT

REFERENCES

1. Roderick, G.L., Everett, R.A., Jr., and Crews, J.H., Jr., "Debond Propagation in Composite-Reinforced Metals", Fatigue of Composite Materials, ASTM STP 569, American Society of Testing and Materials, Philadelphia, 1975, pp.295-306.
2. Brussat, T.R., Chiu, S.T., and Mostovoy, S., "Fracture Mechanics for Structural Adhesive Bonds", AFML-TR-77-163, Air Force Materials Laboratory, 1977.
3. Romanko, J. and Knauss, W.G., "Fatigue Behavior of Adhesively Bonded Joints", Vol. I, AFWAL-TR-80-4037, Air Force Materials Laboratory, 1980.
4. Everett, R.A., Jr., "The Role of Peel Stresses in Cyclic Debonding", Adhesive Age, Vol. 26, No. 5, May 1983, pp. 24-29.
5. Mall, S., Johnson, W.S., and Everett, R.A., Jr., "Cyclic Debonding of Adhesively Bonded Composites", Adhesive Joints: Their Formation, Characteristics, and Testing, K. L. Mittal, Ed; Plenum Press, New York, 1984. pp.639-658.
6. Mall, S. and Johnson, W.S., "Characterization of Mode I and Mixed-Mode Failure of Adhesive Bonds Between Composite Adherends", NASA Technical Memorandum 86355, Feb. 1985.
7. Dattaguru, B., Everett, R.A., Jr., Whitcomb, J.D., and Johnson, W.S., "Geometrically-Nonlinear Analysis of Adhesively Bonded Joints", Journal of Engineering Materials and Technology, ASME, Vol. 106, January 1984, pp.59-65.
8. Rybicki, E.F. and Kanninen, M.F., "A Finite Element Calculation of Stress Intensity Factors by a Modified Crack Closure Integral", Engineering Fracture Mechanics, Vol. 9, No. 4, 1977, pp. 931-938.
9. Johnson, W.S. and Mall, S., "A Fracture Mechanics Approach for Designing Adhesively Bonded Joints", NASA Technical Memorandum 85694, Sept. 1983.

Standard Bibliographic Page

1. Report No. NASA CR- 177990	2. Government Accession No.	3. Recipient's Catalog No.
4. Title and Subtitle INTERACTION OF MIXED MODE LOADING ON CYCLIC DEBONDING IN ADHESIVELY BONDED COMPOSITE JOINTS		5. Report Date October 1985
		6. Performing Organization Code
7. Author(s) S. Mall, M. A. Rezaizadeh, and G. Ramamurthy		8. Performing Organization Report No.
9. Performing Organization Name and Address University of Missouri Department of Engineering Mechanics Rolla, MO 65401-0249		10. Work Unit No.
		11. Contract or Grant No. NAG1-425
12. Sponsoring Agency Name and Address National Aeronautics and Space Administration Washington, DC 20546-0001		13. Type of Report and Period Covered Contractor Report
		14. Sponsoring Agency Code 505-33-33-05

15. Supplementary Notes

Langley technical monitor: Dr. W. S. Johnson

16. Abstract

A combined experimental and analytical investigation of an adhesively-bonded composite joint was conducted to characterize the fracture mode dependence of cyclic debonding. The system studied consisted of graphite/epoxy adherends bonded with EC 3445 adhesive. Several types of specimens were tested which provided the cyclic debond growth rate measurements under various load conditions: mode I, mixed mode I-II, and mostly mode II. This study showed that the total strain-energy-release rate was the governing factor for cyclic debonding.

17. Key Words (Suggested by Authors(s)) Adhesives, fracture mechanics, mixed mode loading, cyclic debonding, composites, bonded joints, cracked-lap-shear specimen	18. Distribution Statement Unclassified-Unlimited Subject Category 24		
19. Security Classif.(of this report) Unclassified	20. Security Classif.(of this page) Unclassified	21. No. of Pages 8	22. Price A02

NASA Langley Form 63 (June 1985)

End of Document